

## Effects of $\text{Br}^-$ and $\text{I}^-$ concentrations on Zn electrodeposition from ammoniacal electrolytes

Zhi-mei Xia<sup>1,2)</sup>, Sheng-hai Yang<sup>1)</sup>, Liang-hong Duan<sup>1)</sup>, and Mo-tang Tang<sup>1)</sup>

1) School of Metallurgy and Environment, Central South University, Changsha 410083, China

2) School of Metallurgical Engineering, Hunan University of Technology, Zhuzhou 412000, China

(Received: 26 December 2014; revised: 29 March 2015; accepted: 30 March 2015)

**Abstract:** The effects of  $\text{Br}^-$  and  $\text{I}^-$  concentrations on the cell voltage, anodic polarization, current efficiency (CE), and energy consumption (EC) of zinc electrodeposition from ammoniacal ammonium chloride solutions were investigated. The surface morphology of zinc deposits was also examined. Scanning electron microscopy (SEM) and X-ray diffraction (XRD) were used to characterize the morphology of zinc deposits and the phase of anodic sediments produced during electrolysis. The results clearly showed that the CE slightly increased from approximately 95.12% in the absence of  $\text{I}^-$  and  $\text{Br}^-$  to 97.08% in the presence of  $10 \text{ g}\cdot\text{L}^{-1} \text{Br}^-$ ; in contrast, the CE significantly decreased to less than 83% in the presence of  $10 \text{ g}\cdot\text{L}^{-1} \text{I}^-$ . The addition of  $\text{Br}^-$  and  $\text{I}^-$  positively affected the EC, which decreased from  $2514 \text{ kW}\cdot\text{h}\cdot\text{t}^{-1}$  to approximately  $2300 \text{ kW}\cdot\text{h}\cdot\text{t}^{-1}$ . The results of anodic polarization measurements showed that the voltage drops were 130 and 510 mV when the concentrations of  $\text{Br}^-$  and  $\text{I}^-$  were  $10 \text{ g}\cdot\text{L}^{-1}$  at a current density of  $400 \text{ A}\cdot\text{m}^{-2}$ , respectively. SEM images showed that the addition of  $\text{Br}^-$  and  $\text{I}^-$  caused different crystal growth mechanisms, which resulted in the production of compact and smooth zinc deposits. The anodic reactions of  $\text{I}^-$  were also studied.

**Keywords:** zinc; electrodeposition; bromide; iodide; ammonium chloride; current efficiency; energy consumption

### 1. Introduction

Approximately 11–20 kg of zinc-bearing blast-furnace dust slurry or electric-arc furnace (EAF) dust is reportedly formed for 1 t of produced steel [1–2]. According to the study of Rütten *et al.* [3], 341.8 million tons of EAF dusts were produced worldwide in 2009, including approximately 48.3 million tons produced in China. Zinc-bearing EAF dusts are first converted into crude zinc oxide via a thermal treatment process and are then subjected to sulfate leaching and subsequent electrowinning to obtain zinc [4]. Before the leaching process, crude zinc oxide should be treated via an alkali wash process to eliminate or reduce the content of impurities, particularly halides, which adversely affect the electrowinning process in acidic sulfate solutions. Consequently, a large amount of wastewater must be treated during this procedure [5].

In the 1990s, the EZINEX<sup>®</sup> process was developed to produce metallic zinc directly from crude zinc oxide with

$\text{NH}_4\text{Cl}$  solution at high temperature (greater than  $70^\circ\text{C}$ ) [6]. Tang's group reported a similar process of treating zinc-containing dusts and low-grade zinc oxide ores in  $\text{NH}_3\text{--NH}_4\text{Cl}$  solution at room temperature [7–10]. During the treatment of zinc-bearing dusts, alkaline gangues and some metallic impurities such as Fe, Al, Si, and Pb are present in raw materials but cannot be extracted from the solution because of its alkalinity. Moreover, zinc electrowinning can be performed in halide-containing solutions. Therefore, a special purification process for the removal of  $\text{F}^-$ ,  $\text{Cl}^-$ , and metallic impurities can be avoided, which greatly reduces the burden of subsequent wastewater treatment and water recycling.

In adapting this method, researchers observed that the current efficiency (CE) and energy consumption (EC) of the electrolytic process were significantly changed by the addition of halide ions. Korbach *et al.* [11] mentioned that particular chromium plating baths can operate at high CEs when  $\text{I}^-$ ,  $\text{Br}^-$ , or  $\text{Cl}^-$  is used as an additive. The authors of

Corresponding author: Sheng-hai Yang E-mail: yangsh@mail.csu.edu.cn

© University of Science and Technology Beijing and Springer-Verlag Berlin Heidelberg 2015

several studies in China have reported that adding halide ions can improve the CE and reduce the EC of the electrolytic preparation process of K<sub>2</sub>FeO<sub>4</sub> [12–13]. Several authors have noted that Cl<sup>-</sup> positively affects the CE and EC of nickel electrowinning and the surface morphologies of nickel-deposits from sulfate electrolytes [14]. Olper and Maccangi [15] have also reported that Br<sup>-</sup> and I<sup>-</sup> can depolarize the anodic reaction during zinc electrodeposition from EZINEX electrolyte and, in turn, significantly decrease the anodic potential. However, to our knowledge, the function and mechanism of Br<sup>-</sup> and I<sup>-</sup> on zinc electrowinning in ammoniacal ammonium chloride solution have not yet been investigated.

The objective of this study is to investigate the effects of Br<sup>-</sup> and I<sup>-</sup> concentrations on the CE, anodic polarization, cell potential, EC, and morphology of zinc deposits during the electrowinning of zinc in ammoniacal ammonium chloride electrolytes. Moreover, the electrochemical mechanisms of Br<sup>-</sup> and I<sup>-</sup> are also investigated.

## 2. Experimental

30 L of electrolyte solution containing 40 g·L<sup>-1</sup> Zn<sup>2+</sup>, 5.0 mol·L<sup>-1</sup> NH<sub>4</sub>Cl, 1.5 mol·L<sup>-1</sup> NH<sub>3</sub>·H<sub>2</sub>O, and small amount of additives was prepared from the reaction of ZnO, NH<sub>4</sub>Cl, and NH<sub>3</sub>·H<sub>2</sub>O (28wt% in water) (Analytical grade, Shanghai Chemistry Reagent Company, China) [16].

Anodic polarization curves were measured using a CHENHUA (Shanghai, China/CHI660C) electrochemical workstation; the measurements were conducted using a conventional three-electrode electrochemical cell at 25°C under atmospheric conditions with a 2.25-cm<sup>2</sup> (1.5 cm × 1.5 cm) platinum plate as the counter electrode and a saturated calomel electrode (SCE) mounted inside a Luggin capillary as the reference electrode. Before each experiment, a 1.0-cm<sup>2</sup> (1.0 cm × 1.0 cm) Ti-RuO<sub>2</sub> plate, which was used as the working electrode, was degreased with acetone and anhydrous alcohol, then washed with bi-distilled water, and finally dried. KBr or KI was added to adjust the Br<sup>-</sup> or I<sup>-</sup> concentration, respectively, in the electrolyte solution. The electrochemical experiments were conducted at a constant scan rate of 5 mV·s<sup>-1</sup>; the scanning potential range was 1.0 to 1.7 V vs. SCE for Br<sup>-</sup>-containing electrolytes and 0.7 to 1.8 V for I<sup>-</sup>-containing electrolytes.

Solutions (1.5 L) of as-prepared electrolytes containing different amounts of KBr and KI were placed in 2.0-L polyvinyl chloride (PVC) electrolytic cells. All electrolytic experiments were conducted at 25°C with a 90-cm<sup>2</sup> Ti plate coated with RuO<sub>2</sub> as the anode, a 100-cm<sup>2</sup> pure Ti plate as

the cathode, an electrode distance of 4 cm, and a cathodic current density of 400 A·m<sup>-2</sup>.

Upon completion of deposition, the cathode was removed from the cell, washed twice with dilute ammonia, rinsed three times with deionized water, and then stripped and dried at 60°C in a vacuum oven for 24 h. A Tescan VEGA II XMH microscope was used to characterize the surface morphology of zinc deposits. X-ray diffraction (XRD) patterns of anodic solid precipitates from I<sup>-</sup>-containing electrolytes were collected on a Rigaku D/max 2550 diffractometer using Cu K<sub>α</sub> radiation (40 kV, 200 mA, λ = 0.154 nm) and a slit width of 0.25°; the samples were scanned over the 2θ range from 10° to 90°.

## 3. Results and discussion

### 3.1. Cell voltage

The effects of the concentrations of Br<sup>-</sup> and I<sup>-</sup> on cell voltage are shown in Figs. 1 and 2, respectively, for an electrodeposition duration of 6 h and a cathodic current density

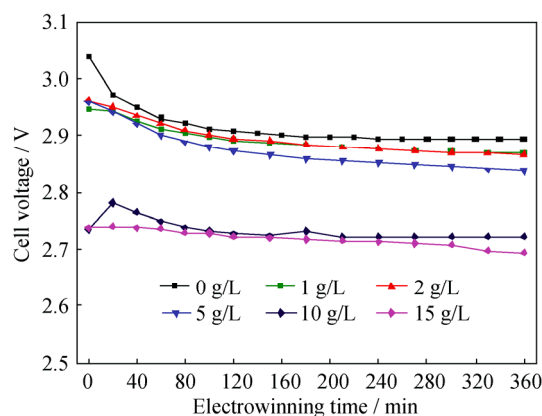


Fig. 1. Change of cell voltage as a function of electrowinning time for electrolytes with various Br<sup>-</sup> concentrations.

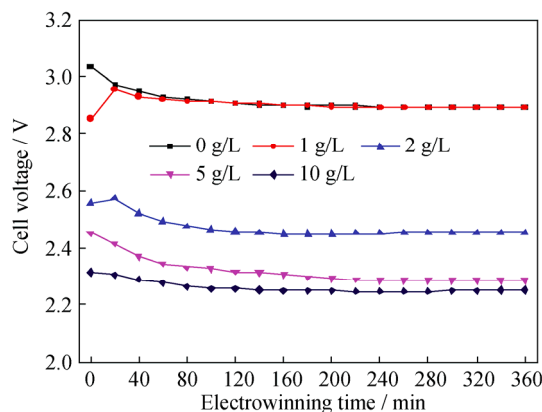


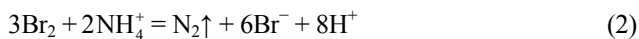
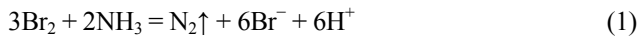
Fig. 2. Change of cell voltage as a function of electrowinning time for electrolytes with various I<sup>-</sup> concentrations.

of  $400 \text{ A}\cdot\text{m}^{-2}$ . The cell voltage decreased with increasing  $\text{Br}^-$  and  $\text{I}^-$  concentrations in the bath. The initial cell voltage decreased from 3.05 to 2.73 V when the  $\text{Br}^-$  concentration was increased from 0 to  $15 \text{ g}\cdot\text{L}^{-1}$ , and the initial cell voltage significantly decreased from 3.05 to 2.26 V when the  $\text{I}^-$  concentration was increased from 0 to  $10 \text{ g}\cdot\text{L}^{-1}$ . One of the most important reasons for this discrepancy in the decrease in cell voltages is that, according to the standard potentials listed in Table 1, both  $\text{Br}^-$  and  $\text{I}^-$  can be oxidized more easily than  $\text{Cl}^-$ . The electrochemical reaction activity on the anode decreases in the order of  $\text{I}_2/\text{I}^- > \text{Br}_2/\text{Br}^- > \text{Cl}_2/\text{Cl}^-$ .

**Table 1. Standard potentials of chlorine, bromine, iodine, and ammonium [17]**

$E_{\text{Cl}_2/\text{Cl}^-}^\ominus$	$E_{\text{Br}_2/\text{Br}^-}^\ominus$	$E_{\text{I}_2/\text{I}^-}^\ominus$	$E_{\text{N}_2/\text{NH}_4^+}^\ominus$
1.395	1.066	0.62	0.275

Alternatively, these phenomena can be caused by an increase in the electrical conductivity of the electrolyte with the addition of  $\text{Br}^-$  and  $\text{I}^-$ . The cell voltage decreased with increasing electrowinning time for each concentration level of  $\text{Br}^-$  and  $\text{I}^-$ , which could be a consequence of the increase in the electrical conductivity of the electrolytes caused by the acid generated during the electrowinning process. The reactions are described as follows:



The average cell voltage as a function of the  $\text{Br}^-$  and  $\text{I}^-$  concentrations is shown in Fig. 3. As expected, the average cell voltage decreased with increasing  $\text{Br}^-$  and  $\text{I}^-$  concentrations. Specifically, in the case of  $\text{I}^-$ , a more significant decrease in cell voltage was observed at concentrations greater than  $1.0 \text{ g}\cdot\text{L}^{-1}$ . The addition of  $15 \text{ g}\cdot\text{L}^{-1} \text{ Br}^-$  and  $10 \text{ g}\cdot\text{L}^{-1} \text{ I}^-$  resulted in the greatest decreases in cell voltage: approximately 195 and 654 mV, respectively.

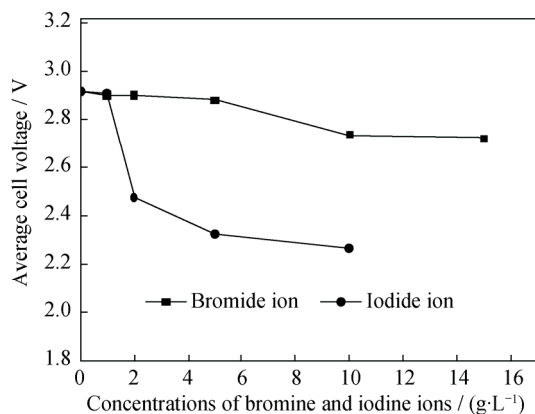


**Fig. 3. Change of average cell voltage as a function of  $\text{Br}^-$  and  $\text{I}^-$  concentrations in the electrolyte.**

### 3.2. Anodic polarization curves

The effects of  $\text{Br}^-$  and  $\text{I}^-$  concentrations on anodic polarization are shown in Figs. 4 and 5, respectively. The addition of  $10 \text{ g}\cdot\text{L}^{-1} \text{ Br}^-$  to the electrolyte resulted in a maximum anodic potential voltage decrease of 130 mV at a current density of  $400 \text{ A}\cdot\text{m}^{-2}$ , thereby indicating that  $\text{Br}^-$  caused the depolarization of the anodic process. The anodic potential drop increased with increasing  $\text{Br}^-$  and  $\text{I}^-$  concentrations in the range of 1 to  $15 \text{ g}\cdot\text{L}^{-1}$  and 1 to  $10 \text{ g}\cdot\text{L}^{-1}$ , respectively (Table 2), which is consistent with the results for the cell voltage.

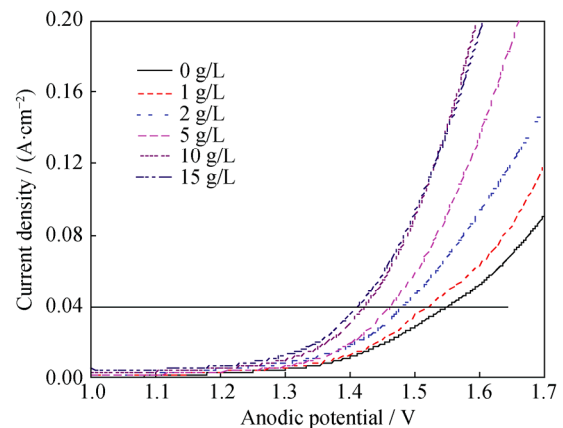


**Fig. 4. Effect of  $\text{Br}^-$  concentration on anodic polarization.**

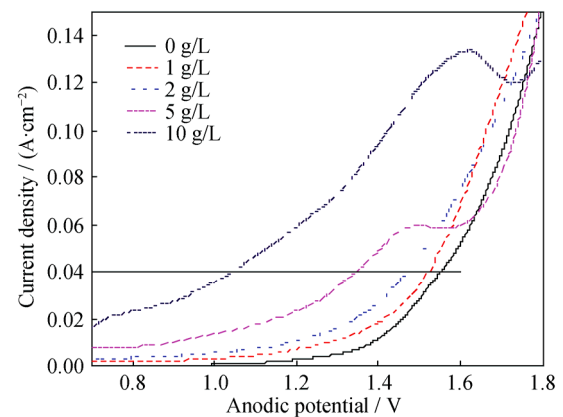


**Fig. 5. Effect of  $\text{I}^-$  concentration on anodic polarization.**

**Table 2. Anodic potential at  $400 \text{ A}\cdot\text{m}^{-2}$  in electrolytes with various  $\text{Br}^-$  and  $\text{I}^-$  concentrations**

Ions	Ion concentration / ( $\text{g}\cdot\text{L}^{-1}$ )					
	0	1	2	5	10	15
$\text{Br}^-$	1.55	1.52	1.48	1.46	1.42	1.41
$\text{I}^-$	1.55	1.52	1.47	1.34	1.04	—

The depolarization caused by  $\text{I}^-$  at a current density of  $400 \text{ A}\cdot\text{m}^{-2}$  was intensified by the addition of  $10 \text{ g}\cdot\text{L}^{-1} \text{ I}^-$ , with a maximum decrease of 510 mV; thus,  $\text{I}^-$  is more effective

tive than Br<sup>-</sup> for depolarizing the anodic reaction. This result is consistent with the rule based on the standard potentials listed in Table 1 that I<sup>-</sup> is oxidized before Cl<sup>-</sup> and Br<sup>-</sup> at an anode. In Fig. 5, a current-density peak was observed with increasing scanning potential when the I<sup>-</sup> concentration in the electrolyte was greater than 5 g·L<sup>-1</sup>. This result was not observed in the polarization curves of Br<sup>-</sup>. A high I<sup>-</sup> concentration resulted in high peak current and high potential. The adsorption of I<sub>2</sub> from I<sup>-</sup> oxidation on the anodic electrode resulted in a decrease in the I<sup>-</sup> concentration, and Cl<sup>-</sup> could be oxidized at a high potential.

During electrolysis with the addition of I<sup>-</sup>, the solution near the anodic surface first became reddish-brown, and brownish-red sediments appeared at the bottom of the anode when the I<sup>-</sup> concentration exceeded 5 g·L<sup>-1</sup>. Moreover, the colorless electrolyte became purple again when the electrolyte was acidified. However, the electrolyte then reverted to being colorless after a certain time. To further understand the anodic reaction mechanism of I<sup>-</sup>, the sediments on the anodic electrode were characterized by XRD; the results are shown in Fig. 6.

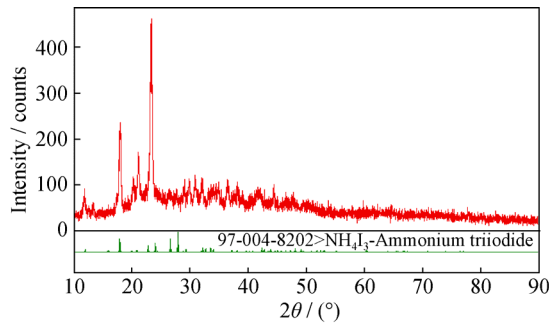


Fig. 6. XRD pattern of sediment from the anodic electrode with the addition of I<sup>-</sup>.

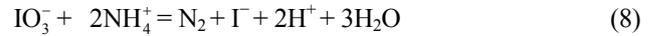
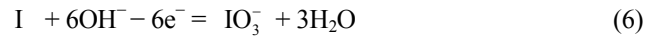
The XRD results showed that the sediment contained NH<sub>4</sub>I<sub>3</sub> (JCPDS #97-004-8202). When I<sup>-</sup> was added to the electrolyte, the ions were oxidized prior to Cl<sup>-</sup> at a lower potential via the following reaction:



However, NH<sub>3</sub> or NH<sub>4</sub><sup>+</sup> cannot be directly reduced to N<sub>2</sub> by I<sub>2</sub>, but the same cannot be said for either Cl<sub>2</sub> or Br<sub>2</sub> because the reducibility of I<sub>2</sub> is much lower than those of Cl<sub>2</sub> and Br<sub>2</sub>. Most of the I<sub>2</sub> combined with I<sup>-</sup> in the solution to form I<sub>3</sub><sup>-</sup>, which eventually led to the formation of NH<sub>4</sub>I<sub>3</sub> according to the following equations:



Alternatively, on the basis of the color change of the electrolyte and gas formation, another reaction mechanism shown in Eqs. (6) to (8) could be involved:



### 3.3. Current efficiency and energy consumption

CE and EC are important performance parameters in electrowinning. The CE for zinc electrodeposition was determined from the mass of the deposits before and after deposition according to the following equation:

$$\eta = \frac{m}{qIt} \times 100\% \quad (9)$$

where  $\eta$  is the current efficiency,  $m$  is the mass of the deposit obtained practically (g),  $q$  is the electrochemical equivalent (the value for zinc is 1.2195 g·A<sup>-1</sup>·h<sup>-1</sup>),  $I$  is the total cell current (A), and  $t$  is the time of electrodeposition (h). The quantity of electricity ( $It$ ) was kept constant for all experiments.

The EC per ton of zinc deposits can be calculated via the following formula using the average cell voltage and CE:

$$W = \frac{V}{q \times \eta} \times 1000 = 820V / \eta \quad (10)$$

where  $W$  represents the energy consumption per ton of zinc deposits (kW·h·t<sup>-1</sup>),  $V$  and  $\eta$  are the average cell voltage (V) and the CE, respectively, and  $q$  is the electrochemical equivalent.

The changes in CE and EC as a function of both Br<sup>-</sup> and I<sup>-</sup> concentrations in the cell electrolyte are shown in Fig. 7. The CE was slightly improved from 95.12% to 97.08% with the Br<sup>-</sup> concentration increasing from 0 to 10 g·L<sup>-1</sup> Br<sup>-</sup>. The energy required for the electrowinning process decreased from 2514 kW·h·t<sup>-1</sup> in the absence of additives to approximately 2309 kW·h·t<sup>-1</sup> with 10 g·L<sup>-1</sup> Br<sup>-</sup>.

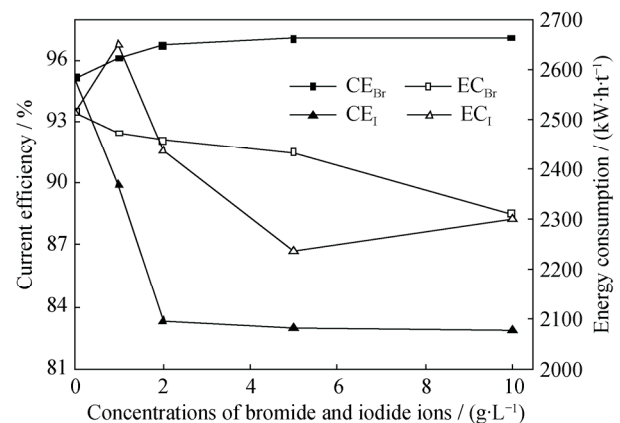
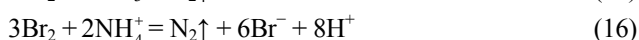
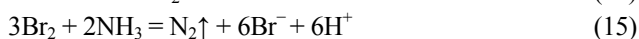


Fig. 7. Change in current efficiency and energy consumption as a function of Br<sup>-</sup> and I<sup>-</sup> concentrations in the electrolyte.

In our previous work, nitrogen was confirmed to be principally released from an anode of titanium coated with ruthenium oxide or from a graphite plate during zinc electro-winning in ammoniacal ammonium chloride solutions according to Eqs. (11) to (13) [18]:



When  $\text{Br}^-$  was added to the electrolyte, the  $\text{Br}^-$  ions were oxidized to  $\text{Br}_2$  prior to the oxidation of  $\text{Cl}^-$  at a lower potential because the redox potential of  $\text{Br}_2/\text{Br}^-$  is lower than that of  $\text{Cl}_2/\text{Cl}^-$ . The generated  $\text{Br}_2$  could also react with  $\text{NH}_3$  or  $\text{NH}_4^+$  in the solution to release  $\text{N}_2$  according to Eqs. (14) to (16):



The solution near the anodic surface became yellow and then quickly became colorless upon the addition of  $\text{Br}^-$ , indicating that  $\text{Br}_2$  was formed. However,  $\text{Br}_2$  was depleted during electrolysis. As a consequence, the CE increased and the cell voltage decreased with the addition of  $\text{Br}^-$  because its redox potential is lower than that of  $\text{Cl}^-$ .

In contrast,  $\text{I}^-$  exhibited a significant negative effect on the CE. The CE significantly decreased from 95.12% in the absence of  $\text{I}^-$  to less than 82.80% with  $10 \text{ g}\cdot\text{L}^{-1} \text{I}^-$ . A small amount of  $\text{I}_3^-$  might have migrated to the cathode and re-

acted with the zinc deposits to form  $\text{ZnI}_2$  according to Eq. (17):



As a result of these side reactions during electrolysis, the CE decreased upon the addition of  $\text{I}^-$ . However, given the significant decrease in cell voltage, the EC also decreased from  $2514 \text{ kW}\cdot\text{h}\cdot\text{t}^{-1}$  to  $2297 \text{ kW}\cdot\text{h}\cdot\text{t}^{-1}$  in the presence of  $10 \text{ g}\cdot\text{L}^{-1} \text{I}^-$  in the electrolyte, despite the decreasing CE.

### 3.4. SEM morphology

The zinc deposits with and without the addition of  $10 \text{ g}\cdot\text{L}^{-1} \text{Br}^-$  exhibited excellent metallic luster, whereas the surface was dull after the addition of  $10 \text{ g}\cdot\text{L}^{-1} \text{I}^-$ . SEM was performed to analyze the surface morphologies of the zinc deposits. Fig. 8 presents SEM micrographs of zinc deposited from electrolyte solutions with various additives. A zinc film was formed from plate-like crystals with different surface morphologies. Many large cavities, small nodules, and long cracks were observed in the zinc deposit obtained from the electrolyte in the absence of  $\text{Br}^-$  and  $\text{I}^-$  (Fig. 8(a)). The zinc deposited from the electrolyte containing  $10 \text{ g}\cdot\text{L}^{-1} \text{Br}^-$  or  $\text{I}^-$  exhibited compact and smooth sheets (Figs. 8(b) and 8(c)). The morphologies of the zinc deposits clearly showed plate-like crystals, and the degree of crystallinity was better than that of the deposits obtained from the electrolyte without  $\text{Br}^-$  and  $\text{I}^-$ . Although the morphologies of all of the zinc deposits maintained a plate-like structure, the primary grain

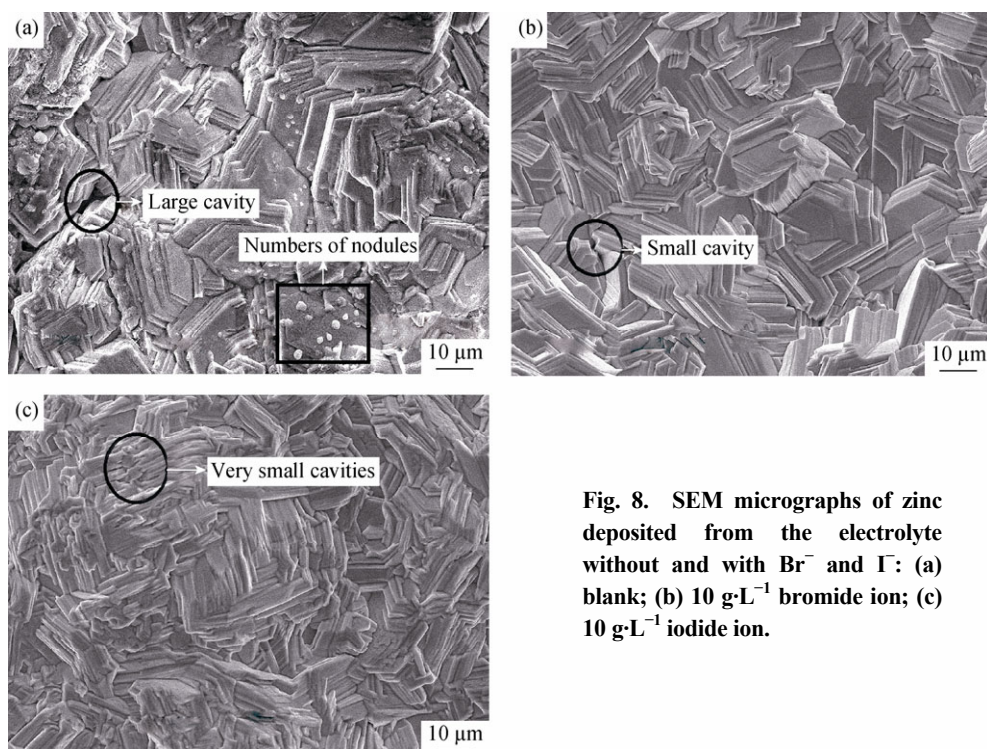


Fig. 8. SEM micrographs of zinc deposited from the electrolyte without and with  $\text{Br}^-$  and  $\text{I}^-$ : (a) blank; (b)  $10 \text{ g}\cdot\text{L}^{-1}$  bromide ion; (c)  $10 \text{ g}\cdot\text{L}^{-1}$  iodide ion.

size, cavities in the primary grains, and particle morphologies differed substantially, indicating that the addition of Br<sup>-</sup> and I<sup>-</sup> played important roles in zinc crystal growth. A particular degree of grain refinement was observed in the zinc deposited from the electrolyte containing 10 g·L<sup>-1</sup> Br<sup>-</sup> or I<sup>-</sup>. On the basis of the irregular edge face of the primary grain of the zinc deposited from the electrolyte with I<sup>-</sup>, the effects of I<sup>-</sup> on the physical characteristics of the deposit were substantially more pronounced than those of Br<sup>-</sup>. A close-packed structure of zinc flakes resulted in compactness and smoothness of the zinc deposits when Br<sup>-</sup> and I<sup>-</sup> were added to the electrolytes. However, further studies on the growth mechanism of zinc crystal nuclei in the presence of Br<sup>-</sup> and I<sup>-</sup> ions are necessary.

#### 4. Conclusions

(1) The CE of zinc electrowinning increased from 95.12% without Br<sup>-</sup> in the electrolyte to greater than 97% when 10 g·L<sup>-1</sup> Br<sup>-</sup> was present. In the case of I<sup>-</sup>, the CE decreased significantly from 95.12% to 82.80% over the entire concentration range of 0 to 10 g·L<sup>-1</sup>, which was attributed to side reactions at the cathode. The addition of Br<sup>-</sup> and I<sup>-</sup> decreased the EC from 2514 kW·h·t<sup>-1</sup> to approximately 2300 kW·h·t<sup>-1</sup>.

(2) The presence of Br<sup>-</sup> and I<sup>-</sup> in the electrolyte resulted in compact and smooth zinc deposits. Br<sup>-</sup> and I<sup>-</sup> facilitated the deposition of close-packed zinc with few and small cavities and no nodules, unlike the zinc deposited in the absence of Br<sup>-</sup> and I<sup>-</sup>.

(3) The positive effects of Br<sup>-</sup> and I<sup>-</sup> ions on cell voltage and EC were attributed to anodic depolarization. When the concentration of Br<sup>-</sup> or I<sup>-</sup> was 10 g·L<sup>-1</sup>, the maximum voltage drop was 130 mV or 510 mV at a current density of 400 A·m<sup>-2</sup>, respectively. However, a high concentration of I<sup>-</sup> can result in the formation of NH<sub>4</sub>I<sub>3</sub> on the anodic surface and IO<sub>3</sub><sup>-</sup> in the electrolyte, which negatively affects the electrodeposition process.

#### Acknowledgements

This work was supported by the National Basic Research Program of China (No. 2014CB643404) and by the National Natural Science Foundation of China (Nos. 51274094 and 51374254).

#### References

[1] T. Suetens, B. Klaasen, K. Van Acker, and B. Blanpain, Comparison of electric arc furnace dust treatment technolo-

- gies using exergy efficiency, *J. Clean. Prod.*, 65(2014), p. 152.
- [2] M. Liebman, The current status of electric arc furnace dust recycling in North America, [in] *Recycling of Metals and Engineered Materials*, Hoboken, 2000, p. 237.
- [3] J. Rütten, C. Frias, G. Diaz, D. Martin, and F. Sanchez, Processing EAF dust through Waelz Kiln and ZINCEXTM solvent extraction: the optimum solution, [in] *European Metallurgical Conference*, Dusseldorf, 2011, p. 1673.
- [4] A.D. Zunkel, Recovering zinc and lead from electric arc furnace dust: a technology status report, [in] *Recycling of Metals and Engineered Materials*, Hoboken, 2000, p. 227.
- [5] S.S. Chabot and S.E. James, Treatment of secondary zinc oxides for use in an electrolytic zinc plant, [in] *Recycling of Metals and Engineered Materials*, Hoboken, 2000, p. 739.
- [6] M. Olper and M. Maccagni, Electrolytic zinc production from crude zinc oxides with the Ezinex<sup>®</sup> process, [in] *Recycling of Metals and Engineered Materials*, Hoboken, 2000, p. 269.
- [7] M.T. Tang and S.H. Yang, Electrowinning zinc in the system of Zn( )-NH<sub>3</sub>-NH<sub>4</sub>Cl-H<sub>2</sub>O and mechanism of anodic reaction, *J. Cent. South Univ. Technol.*, 30(1999), No. 2, p. 153.
- [8] R.X. Wang, M.T. Tang, W. Liu, S.H. Yang, and W.H. Zhang, Leaching of low-grade zinc oxide ore in NH<sub>3</sub>-NH<sub>4</sub>Cl-H<sub>2</sub>O system for production of electrolytic zinc, *Chin. J. Process Eng.*, 8(2008), Suppl. 1, p. 219.
- [9] B.P. Zhang, M.T. Tang, and S.H. Yang, Treating zinc oxide ores using ammonia-ammonium chloride to produce electrolysis zinc, *J. Cent. South. Univ. Technol.*, 34 (2003), No. 6, p. 619.
- [10] S.H. Ju, M.T. Tang, S.H. Yang, and Y.N. Li, Dissolution kinetics of smithsonite ore in ammonium chloride solution, *Hydrometallurgy*, 80(2005), No. 1-2, p. 67.
- [11] W.C. Korbach, N.J. William, Howell, H. McMullen, E. Warren, and Brunswick, *High Performance Electrodeposited Chromium Layers*, American Patent, Appl. 4828656, 1987.
- [12] W.C. He, G.Q. Liu, W. Cui, and Y. Tang, Effects of potassium iodide additive on direct electrosynthesis of potassium ferrate, *Inorg. Chem. Ind.*, 43(2011), No. 2, p. 20.
- [13] W.H. Yang, D.Q. Bi, Y. Zhou, H.H. Wang, and X.R. Lan, Selection of addition in the process of electrochemical synthesizing of K<sub>2</sub>FeO<sub>4</sub>, *Electrochemistry*, 13(2007), No. 4, p. 445.
- [14] A.M. Alfantazi and A. Shakshouki, The effects of chloride ions on the electrowinning of nickel from sulfate electrolytes, *J. Electrochem. Soc.*, 149(2002), No. 10, p. C506.
- [15] M. Olper and M. Maccagni, From C.Z.O. to zinc cathode without any pre-treatment, [in] *Proceedings of the EZINEX Process, Lead and Zinc 2008*, Durban, 2008, p. 85.
- [16] Z.M. Xia, S.H. Yang, M.T. Tang, T.Z. Yang, Z.H. Liu, C.B. Tang, J. He, and X.L. Deng, Cycle leaching of low grade zinc oxide ores in MACA system for preparing zinc, *Chin. J. Nonferrous Met.*, 23(2013), No. 12, p. 3455.
- [17] A.J. Bard, R. Parsons, and J. Jordan, *Standard Potentials in Aqueous Solution*, CRC Press, New York and Bessel, 1985, p. 221.
- [18] S.H. Yang, *Theory and Application Studies on Preparing High Purity Zinc in the System of Zn(II)-NH<sub>3</sub>-NH<sub>4</sub>Cl-H<sub>2</sub>O* [Dissertation], Central South University, Changsha, 2003, p. 32.